277

NO

MSC INTERNAL NOTE 66-EG-16

PROJECT APOLLO

AN ERROR ANALYSIS OF ONBOARD PRIMARY NAVIGATION SYSTEMS FOR THE LUNAR EXCURSION MODULE

Prepared by: Jerold H. Suddath
J. H. Suddath

Robert H. Kidd III
R. H. Kidd, III

Approved: Kenneth J. Cox
Kenneth J. Cox
Chief, Systems Analysis Branch

Approved: R G Chilton
Robert G. Chilton, Deputy Chief
Guidance and Control Division

NATIONAL AERONAUTICS AND SPACE ADMINISTRATION

MANNED SPACECRAFT CENTER

HOUSTON, TEXAS

April 15, 1966

SUMMARY

A study has been made to determine the accuracies which could be expected from onboard primary navigation systems for the Lunar Excursion Module following the concentric flight plan. Emphasis was placed on comparing a Rendezvous Radar with an Optical Tracker as a source of navigational information. The comparison was drawn from error analyses of the navigation systems as they would function in various phases of the concentric flight plan. The results of the investigation indicate that there is little difference between Rendezvous Radar and Optical Tracker performance in the primary navigation system in terms of navigation accuracy or fuel requirements. Furthermore, for either sensor, the effect of reduced accuracy and the effect of varying the measurement sampling period on navigation accuracy are of little significance.

INTRODUCTION

The purpose of this study was to compare a Rendezvous Radar with an Optical Tracker as a source of navigational information in an onboard primary navigation system for the Apollo Lunar Excursion Module (LEM). The comparison was drawn from error analyses of one system with an Optical Tracker, and another system with a Rendezvous Radar. Included in this comparison are the effects of sun and moon interference on the sensors, inertial measurement unit (IMU) alinement accuracies of the two systems, command-service module (CSM) ephemeris uncertainties, and navigation base misalinement. An adequate treatment of these effects, as applied to the Concentric Flight Plan (CFP) for rendezvous, constitutes the difference between this investigation and the error analysis reported earlier in reference 1. The study reported in reference 1, further, considered only direct transfers to rendezvous.

The error analyses were performed by using a digital computer to calculate the covariance matrix for the errors of a navigation system (using either the radar or tracker) as a function of time along the trajectories of interest. It was assumed that the navigation system would estimate the state (position and velocity) of the LEM measured relative to the CSM, and that the estimation would be done with a Kalman type filter (reference 2).

Results are presented in the form of time histories of RMS relative position and velocity estimation uncertainties for the trajectories considered and a table giving estimates of the ΔV required to compensate for injection errors for the nominal and late launch.

SCOPE OF THE STUDY

To compare a Rendezvous Radar with an Optical Tracker as a source of navigational information for the LEM, it was necessary to consider the salient characteristics of the overall LEM mission. In this study, the LEM mission was taken to be that of following the CFP (described in reference 3). The nominal sequence of events on the CFP was taken to be the following:

a. LEM separation from CSM

b. Hohmann descent

c. Powered descent

d. Landing

e. Nominal launch

f. 90^{o} burn to adjust apocynthion

g. Circularization

h. Transfer maneuver

i. Terminal rendezvous

In addition to the nominal sequence of events, there were the following contingencies which had to be examined (reference 4):

a. Abort 12 minutes after LEM separation; 70 degree direct transfer to rendezvous.

b. Abort 35 minutes after LEM separation; 140 degree direct transfer to rendezvous.

c. Abort from start of powered descent.

d. Abort from hover.

e. Late launch.

The necessity of having to consider all these phases of the mission arose because there are physical limitations on both sensors which restrict their ability to track. For example, the Optical Tracker cannot track if the angle between the lines-of-sight to the sun and to the CSM is less than some critical value which is shown in figure 1 as a function of relative range. Also, the tracker cannot track the CSM against a fully illuminated lunar background at ranges greater than 40 n.m. Moreover, neither the tracker nor the radar can track at ranges greater than 400 n.m. Thus, every phase of the mission had to be examined to see if these limitations created any major problem areas.

METHOD OF ANALYSIS

The error analyses were performed by using a digital computer to calculate the covariance matrix for the errors of a navigation system (using either radar or tracker) as a function of time along the trajectories of interest. The computer program, which was used, is described in the appendix.

The RMS relative position uncertainty was obtained by taking the square root of the sum of the first three diagonal elements of the covariance matrix. Similarly, the RMS relative velocity uncertainty was obtained by taking the square root of the sum of the second three diagonal terms of covariance matrix. Navigational measurements were simulated only in the sense of computing their effects on the statistics of the estimation process.

To do this type of error analysis, it is necessary to have certain a priori statistics given. Also, it is necessary to have statistical error models for the radar, tracker, accelerometers, CDU, platform drive and IMU and NAV Base misalinements. The error models used in this study are discussed in the next section.

ERROR MODELS

Optical Tracker - The model used for the optical tracker is described in the following way. It was assumed that the tracker would measure the azimuth and elevation angles of the CSM relative to an inertial coordinate system (the IMU). The sun interference constraint is plotted in figure 1. Other pertinent data are given in the following table.

Bias ($1\ \sigma$) = .2 mr

Noise ($1\ \sigma$) = .15 mr

For the tracker, specification data indicated that NAV Base misalinement errors were negligible.

Rendezvous Radar - The model used for the radar is described as follows. It was assumed that the radar would measure either relative range or relative range-rate, and shaft and trunion angles (defining the line-of-sight to the CSM) relative to the NAV Base. Pertinent data for the radar are given in the following table.

Range bias ($1\ \sigma$) = 500 feet

Range Noise ($3\ \sigma$) = greater of $\frac{1}{4}\%$ or 300 feet

Range Rate Bias ($1\ \sigma$) = 1 ft./sec.

Range Rate Noise (3σ) = greater of $\frac{1}{4}\%$ or 1 ft./sec.

Angle Bias (3σ) = 7 mr (including NAV Base misalinement)

Angle Noise (3σ) = 2 mr for range $<$ 200 n.m. linearly increasing to 4 mr at 400 n.m.

For the Rendezvous Radar, the NAV Base misalinement errors (specification values) are significant to the point where vehicle attitude must be known to represent the errors in a measurement. This being the case, vehicle attitude profiles had to be assumed in the simulations of the radar.

The nominal attitude profile used in all radar simulations is described as follows:

a. No roll or yaw; LEM X-Z plane always coincident with orbital plane (see figure 2).

b. Pitch vehicle so as to maintain LEM Z-axis along line-of-sight from LEM to CSM.

The reasons for selecting this attitude profile are the following:

a. With the vehicle Z-axis along the line-of-sight, the radar is always essentially boresighted down the Z-axis. This tends to minimize the radar boresight drift error since it is a function of the shaft and trunion angles which in this case are nominally zero.

b. Since the normal field-of-view for the astronauts is in the direction of the LEM Z-axis, this attitude profile keeps the CSM in their field-of-view at all times.

c. This attitude profile would also simplify the mechanization of the onboard navigation system.

IMU Errors - When a ΔV maneuver is made, the errors in the estimate of the applied ΔV increase the uncertainties in the estimate of the vehicle velocity. Since the IMU measures the applied ΔV, the error estimating the applied ΔV comes from the IMU errors. Therefore, after a ΔV maneuver, the covariance matrix for the error in the navigational estimate must be updated in accordance with the error model for the IMU. The data used for the IMU errors (specification values) are given in the following table:

Accelerometer bias (1σ) = .00656 ft./sec.

Accelerometer scale factor (1σ) = 100 PPM

Alinement: LORS (1σ) = .2 mr

AOT (1σ) = 1 mr

RESULTS AND DISCUSSION

Using the error models presented in the previous sections, and the computer program described in the appendix, various trajectories associated with the concentric flight plan were simulated. For each trajectory the three basic cases considered were:

1. Navigational information provided by Optical Tracker measuring azimuth and elevation angles.

2. Navigational information provided by Rendezvous Radar measuring shaft and trunion angles and range.

3. Navigational information provided by Rendezvous Radar measuring shaft and trunion angles and range rate.

The results of the simulations are discussed in the following sections:

Nominal Launch - The geometry of the CFP nominal launch trajectory is represented in Figure 3. The trajectory consists of the following sequence of events:

1. Powered ascent from launch site (taken to be 0° long., 0° lat.) to ascent injection.

2. Coast through approximately 90° central angle.

3. At approximately 90° a ΔV maneuver is made to adjust the altitude and longitude of apocynthion.

4. Circularization of the orbit at apocynthion and coast to transfer.

5. At the transfer point a ΔV maneuver is made to put the LEM on a 140° direct transfer to rendezvous.

The simulation of this phase of the CFP was initiated at ascent injection. It was assumed that navigational measurements would be made every three minutes provided the constraints on the sensors were satisfied. Results of the simulations are shown in figure 4. Figure 4a is a semi-log plot of the RMS relative position uncertainties in feet versus time after ascent injection in minutes.

The curve at the top of the figure is for the case where no measurements are made throughout the trajectory. It is seen that for this case, the RMS relative position uncertainty begins at about 3700 ft. and simply grows to about 6800 ft at the time of rendezvous.

The curve at the bottom of the figure is for the case where the Optical Tracker was used to make measurements. It should be noted that the initial uncertainty for this case is about 400 ft. less than for the other cases ploted on the figure. This results because prior to launch, the platform

is realined, and the alinement with the Optical Tracker system is more accurate than the corresponding alinement with the Radar System. Therefore, when the alinement errors are propagated through the powered ascent, the tracker system has smaller injection errors than the radar system.

It should be pointed out that the Optical Tracker does experience sun interference, which is indicated in the figure as occurring at 67 min. and lasting until 78 min. after injection. This trajectory was computed assuming that the sun elevation angle (relative to the lunar local horizontal) at the landing point was 45°, and the lunar stay time was 36 hours. However, other trajectories were computed with the elevation angle being varied up from an elevation of 15° and no significant difference was noted in the performance of the tracker system. Therefore, this case was presented as being typical of any sun elevation angle currently being considered for the CFP, and it was concluded that sun interference with the Optical Tracker is not a problem on the nominal launch.

The two curves in the middle of the figure are for the two cases where the Rendezvous Radar was the sensor. In both cases shaft and trunion angles were measured so that the cases differ only in that range was the third measurable in one case whereas range-rate was the third measurable in the other case. It should be clear that the two types of radar differed very little in terms of the navigational accuracy they provided.

Figure 4b is a semi-log plot of the RMS relative velocity uncertainties in feet per second versus time after injection in minutes. The description of this plot is virtually the same as the preceding description of figure 4a.

It should be pointed out that the "lumps" on the radar curves are due to out-of-plane errors. This is easily seen by examination of figure 4c which is a plot of the components of the relative position uncertainties along the line-of-sight (LOS), out-of-plane, and in the orbital plane normal to the LOS. Although the plot is for the case where no measurements are made the periodic character of the out-of-plane error is very evident in the radar errors plotted in figure 4a.

In the navigation system of this study, the relatively large radar out-of-plane errors were due to a NAV Base misalinement bias. If necessary, the error could be reduced substantially by simply estimating any difference between the radar and tracker accuracies, it would impose some additional computational requirements on the radar system. Overall comparison of the curves on figures 4a and 4b shows that there is little difference in navigation accuracy using either the Optical Tracker or the Rendezvous Radar in the primary navigation mode.

Late Launch - The geometry and sequence of events for the CFP late launch trajectory are essentially the same as the nominal launch trajectory. The only substantial difference is the position of the CSM at launch. Figure 5 is a semi-log plot of the RMS relative position uncertainty in feet versus time after injection in minutes. The description of this plot is similar to the description of figure 4a.

It should be noted that during the first 21 minutes of the late launch trajectory, neither the Optical Tracker nor the Radar can make measurements. This is due to the fact that the relative range during this period is greater than 400 n.m.

Once again the Optical Tracker experienced sun interference, but it was found that interference is not a problem on the late launch.

Abort Trajectory Results - The geometry of the abort from start of powered descent is shown in figure 6.

A semilog plot of the relative position error for an abort 12 minutes after LEM/CSM separation is shown in figure 7. This is a direct transfer through 70°. The time of abort is indicated on the plot, and it should be clear from the legend which curve goes with which system.

The relative position error for an abort 35 minutes after LEM/CSM separation is shown in figure 8, using a direct transfer through 140°. This plot is virtually the same as the other abort. There is no sun interference on the tracker for this and the above abort case for elevation at the landing site corresponding to 15° to 45°. Figure 9 shows relative position error for an abort from start of powered descent. The only thing different about this plot is the moon interference toward the end of the trajectory. The error in the optical tracker increases slowly during the period of moon interference, but once track is reestablished, the error comes back down. Therefore, moon interference with the tracker does not appear to be a problem. The reason for the relatively large buildup of errors during the first portion of the trajectories is as follows: During the first part of the trajectory, the optical tracker is hampered by the fact that there is a low line-of-sight rate. Whenever this is the case, the tracker does not get a lot of information and the error tends to grow. The reason for the radar error growing at the beginning of the trajectory is the rather large bias in the range initially, and even though the bias is being estimated, it takes a certain amount of information coming in to get an estimate of this bias. Therefore, during the first part of the trajectory, most of the information is going into the estimation of bias and very little into the estimation of the state. Once the bias estimate becomes fairly good, the radar errors tend to decrease until the point is reached in the trajectory where relative range becomes quite large. Since the noise in the radar range measurement is a function of the range, the noise is going up and therefore causing errors to go up during the middle portion of the trajectory.

There is little difference between the navigation accuracies obtained with radar and optical tracker for the abort trajectories considered. This is consistent with the statement made earlier for the nominal launch trajectory.

Effect of Sampling Period - The effect of sampling period on relative position error for the optical tracker for the nominal launch trajectory is shown in figure 10. The solid curve shows the error if one measurement is made every three minutes whereas the dashed curve shows the error if there is only one measurement made every nine minutes. After a measurement is made on the nine-minute sampling period case, the error is very close to the three-minute sampling period curve. As long as we are aware of this and know that we should only look at our estimate immediately after making a measurement, then we can conclude that increasing the sample period does not degrade the accuracy of the system very much.

The effect of sampling period on relative position error for the range radar shown in figure 11 is very similar to the effect of sampling period on the optical tracker (compare figure 11 with figure 10), and the same conclusions as were drawn before are pertinent in this case.

Effect of Sensor Accuracy - The effect of optical tracker accuracy on the relative position errors on the nominal launch trajectory is shown in figure 12. The dashed curve is the performance we get if the tracker has the specification value for the noise whereas the solid curve is the error if the errors were three times the specification values. While there is some degradation in the performance of the system with the errors being increased by the factor of three, the degradation does not appear significant.

The effect of range radar accuracy on relative position errors for nominal launch is shown on figure 13. The dashed curve is for the radar with the specification values. The solid curve is for three times the specification values and the dotted curve is for specification noise but the angle bias is reduced to one milliradian. Once again, there is some degradation when the noise and bias are three times the specification values, but since the errors are probably significant only at the end of the trajectory, the degradation does not seem to be very serious.

Characteristic Propulsive Fuel Requirements - Estimates of the ΔV required to compensate for injection errors are shown in figure 14. These numbers were computed by assuming that in-plane errors would be taken out at the 90° burn and that the out-of-plane errors would be taken out at the transfer point. The approximate nature of the ΔV's presented here is due to the fact that the statistics of the individual ΔV's are not easily represented analytically. Approximations were made so that an analytical solution could be obtained from a more tractable distribution by linearizing about the nominal ΔV, computing the required partial derivatives, and assuming perfect estimation accuracy at the 90° maneuver. Presented here

are the means, denoted by μ, and the standard deviations denoted by σ, for both the nominal and late launches, and for both LORS and the Rendezvous Radar. It can be seen from the numbers that there is very little difference in the ΔV penalty between the two types of systems.

CONCLUDING REMARKS

A study was made to determine the accuracies which could be expected from onboard primary navigation systems for the Lunar Excursion Module following the concentric flight plan. Emphasis was placed on comparing a Rendezvous Radar with an Optical Tracker as a source of navigational information. The comparison was drawn from error analyses of the navigation systems as they would function in various phases of the concentric flight plan. The results of the investigation indicate that there is little difference between rendezvous radar and optical tracker performance for specification error models in the primary navigation system in terms of navigation accuracy or fuel requirements. It was found that sun interference has little effect on the accuracy of the primary system with the optical tracker. Furthermore, the effects of measurement sampling period and degraded systems have little significance.

REFERENCES

1. Kidd, R. H., Carney, T. M., Suddath, J. H.; Project Apollo - Linearized Statistical Error Analysis of Apollo Lunar Excursion Module Ascent and Rendezvous for Comparison of Several Measurement Schemes, MSC Internal Note 65-EG-11, March 1965

2. Kalman, R. E.; A New Approach to Linear Filtering and Prediction Problems, Journal of Basic Engineering, March 1960

3. Alexander, J. D. and Kehl, R. P.; LEM Nominal Concentric Ascent Technique for Lunar Landing Mission, MSC Internal Note 65-FM-170, January 1966

4. Price, Charles R.; Description of the LEM Orbital Maneuvers for a Typical Apollo Lunar Landing Mission, MSC Internal Note 66-EG-14, April 1966

ANGLE BIAS (1σ) = .2 M r

RANDOM ANGLE (3σ) = .45 M r

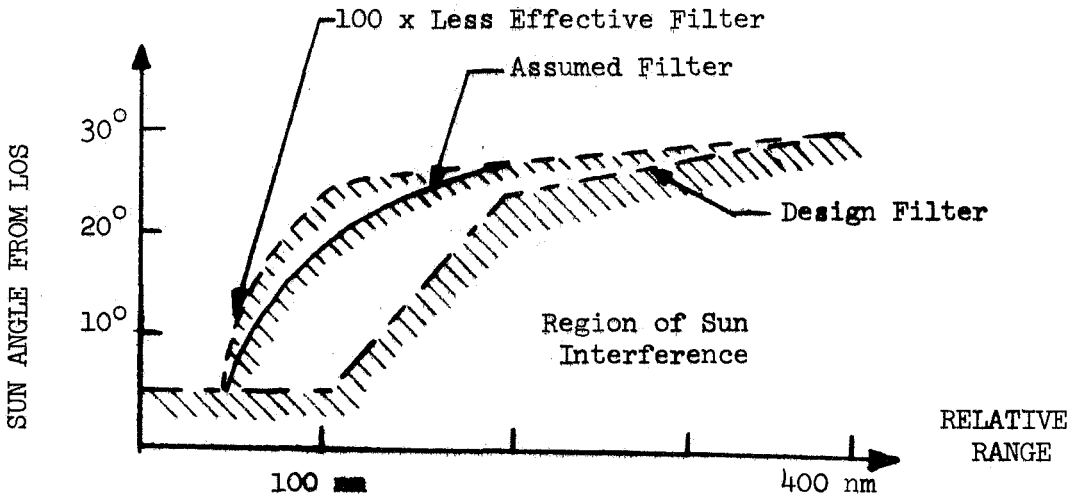

FIGURE 1 OPTICAL TRACKER ERROR MODEL AND SUN ANGLE CONSTRAINT

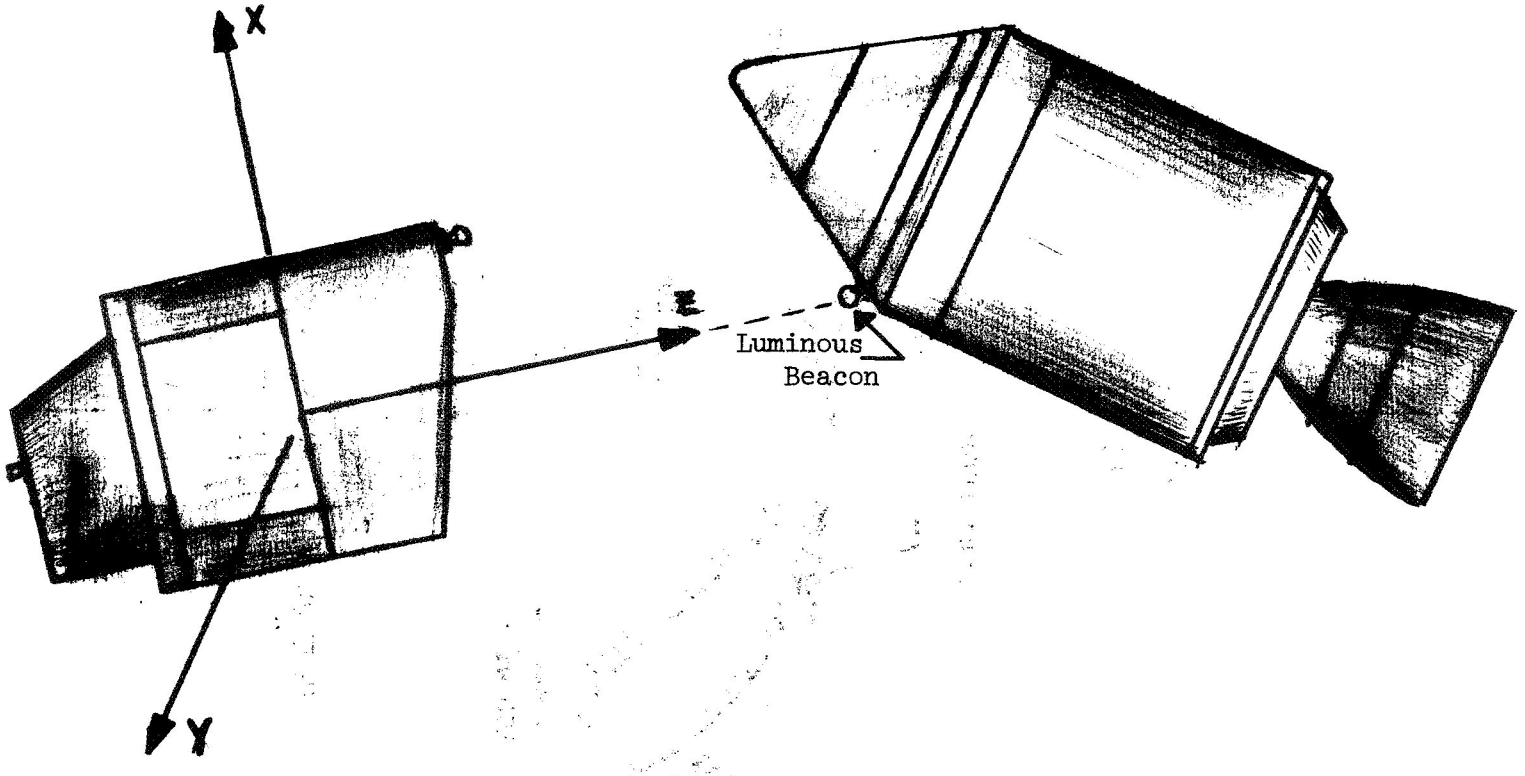

FIGURE 2 LEM ATTITUDE PROFILE

NASA-S-66-2959 APR 4

CONCENTRIC FLIGHT PLAN

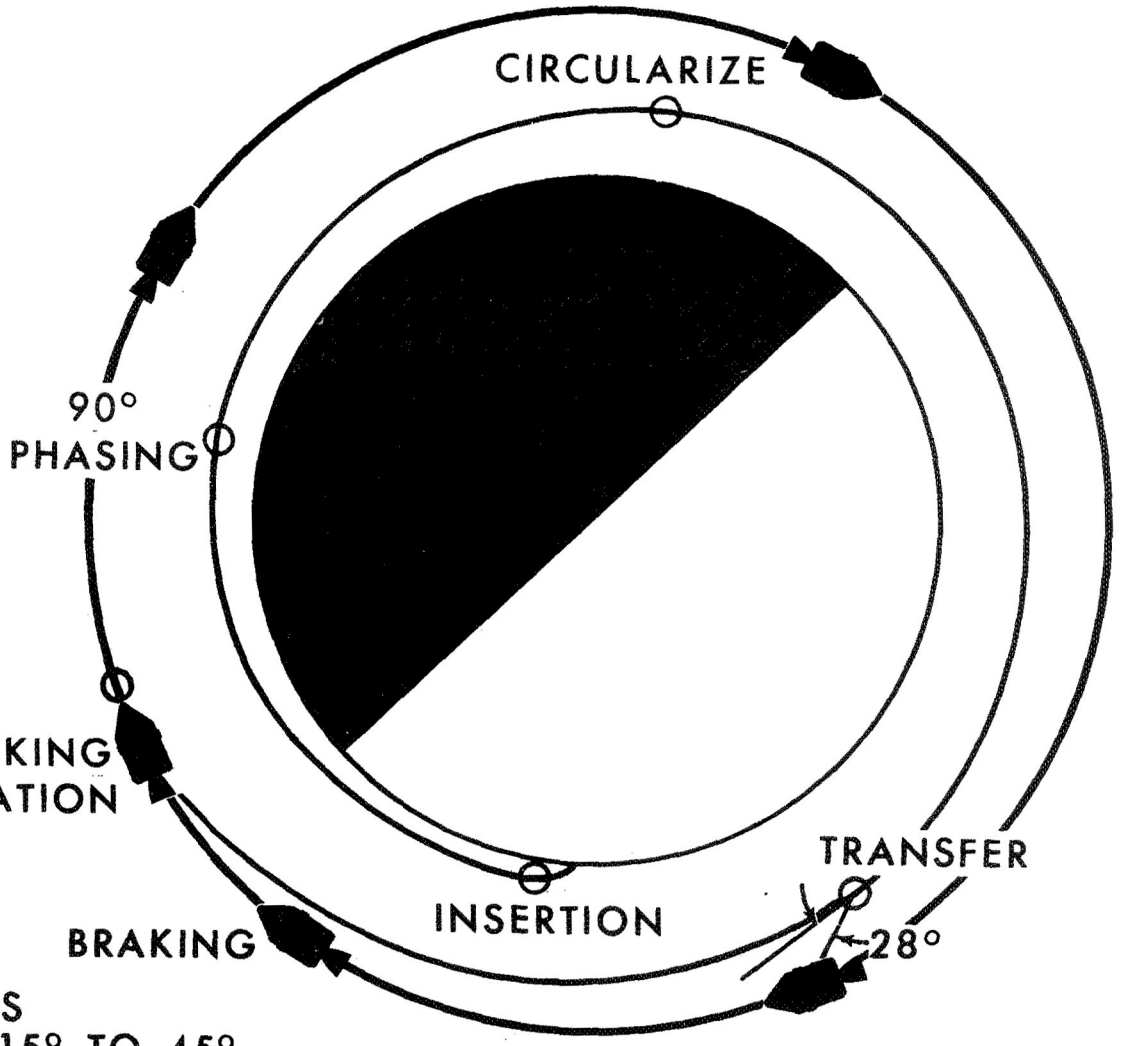

SUN ELEVATION ANGLES
AT LANDING SITE: 15° TO 45°

CIRCULARIZATION
ALTITUDES: 30 TO 65 N MI

FIGURE 3

NASA-S-66-3122 APR 8

RELATIVE POSITION ERROR (NOMINAL LAUNCH)

SUN ELEVATION = 45°
SAMPLING PERIOD = 3 MIN

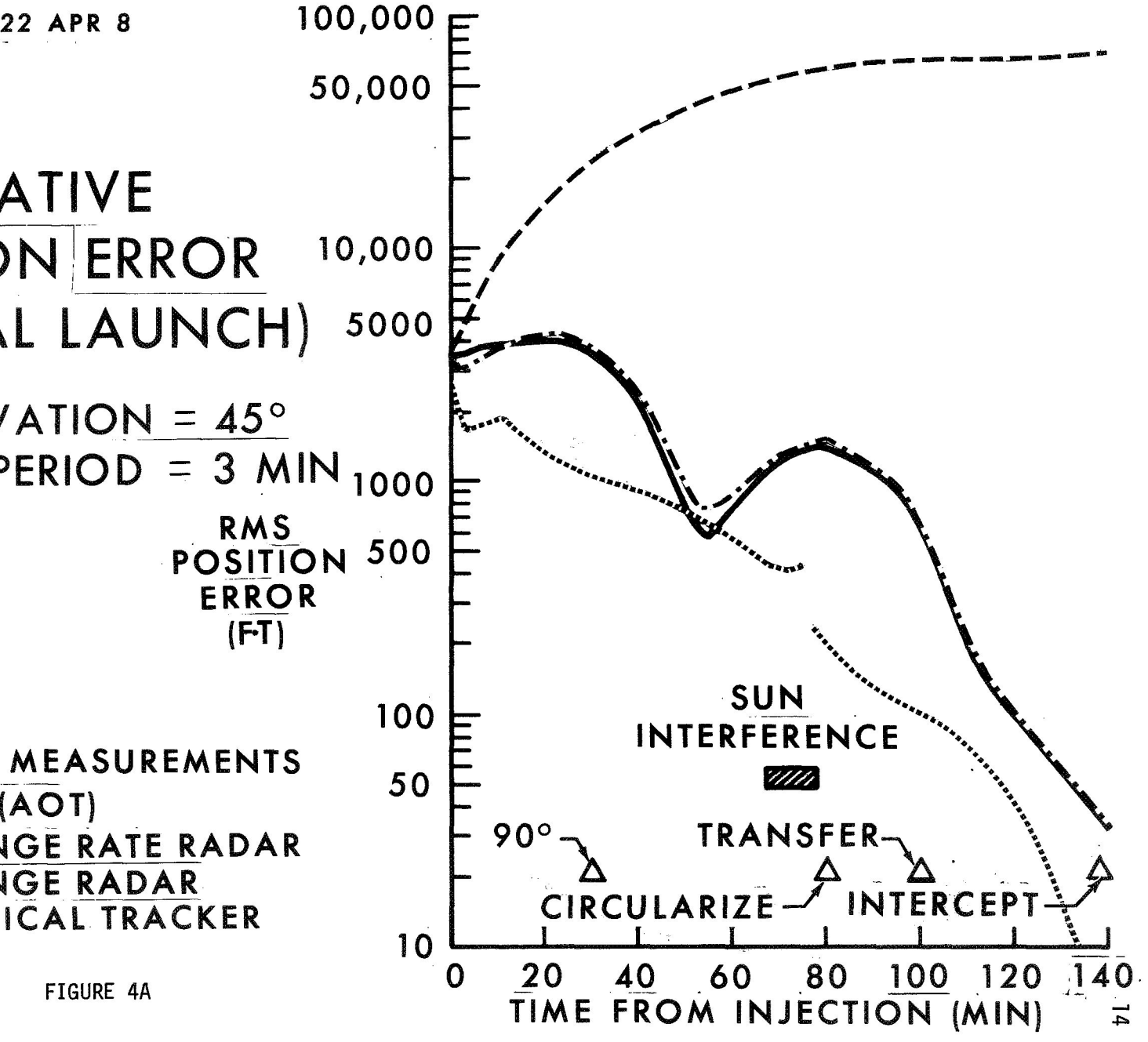

FIGURE 4A

NASA-S-66-2972 APR 4

RELATIVE VELOCITY ERROR (NOMINAL LAUNCH)

SUN ELEVATION = 45°
SAMPLING PERIOD = 3 MIN

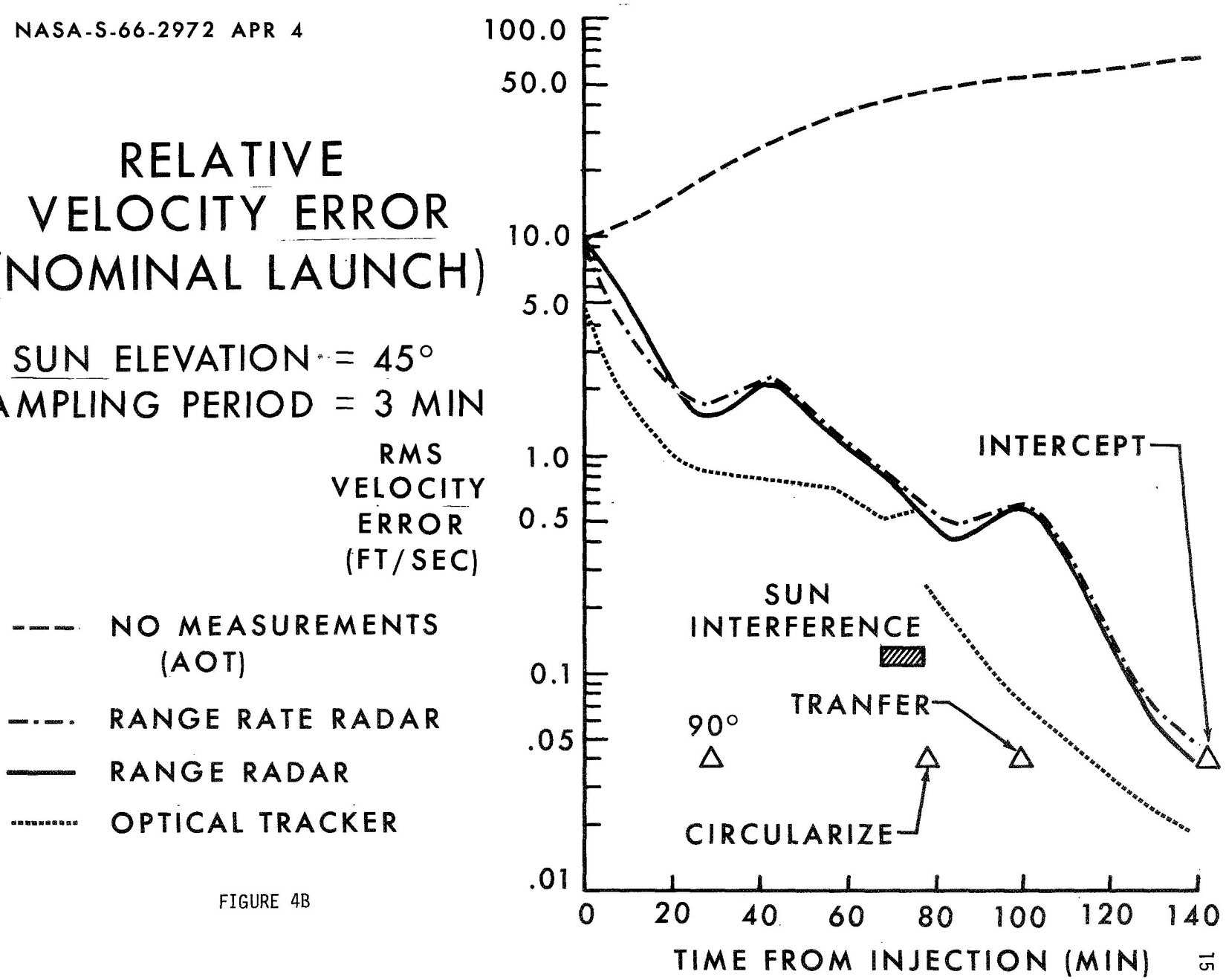

FIGURE 4B

NASA-S-66-2998 APR 4

RELATIVE POSITION ERROR (LATE LAUNCH)

SUN ELEVATION = 45°

SAMPLING PERIOD = 3 MIN

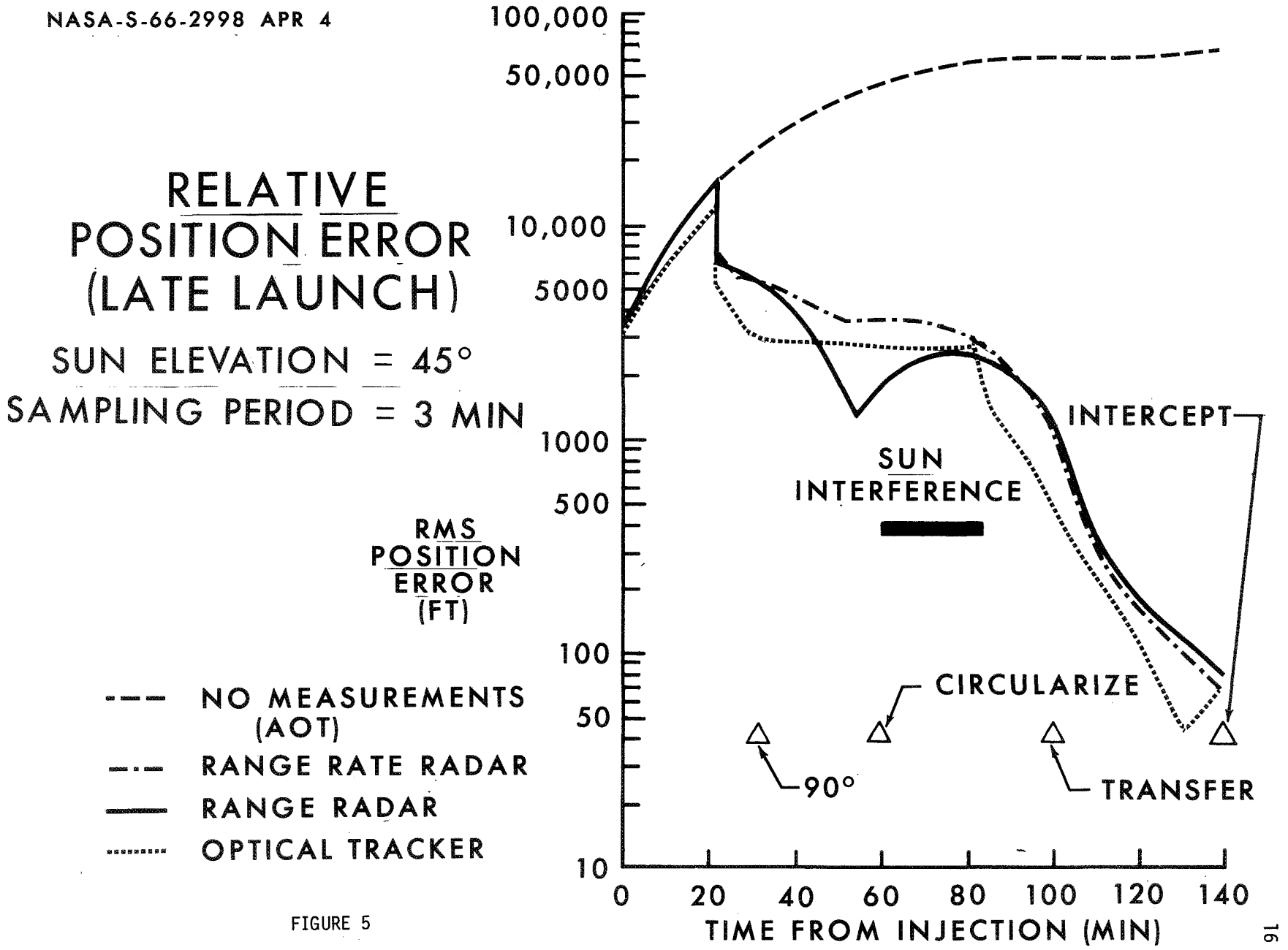

FIGURE 5

NASA-S-66-3129 APR 8

LEM/CSM RELATIVE INERTIAL POSITION, ABORT START POWERED DESCENT

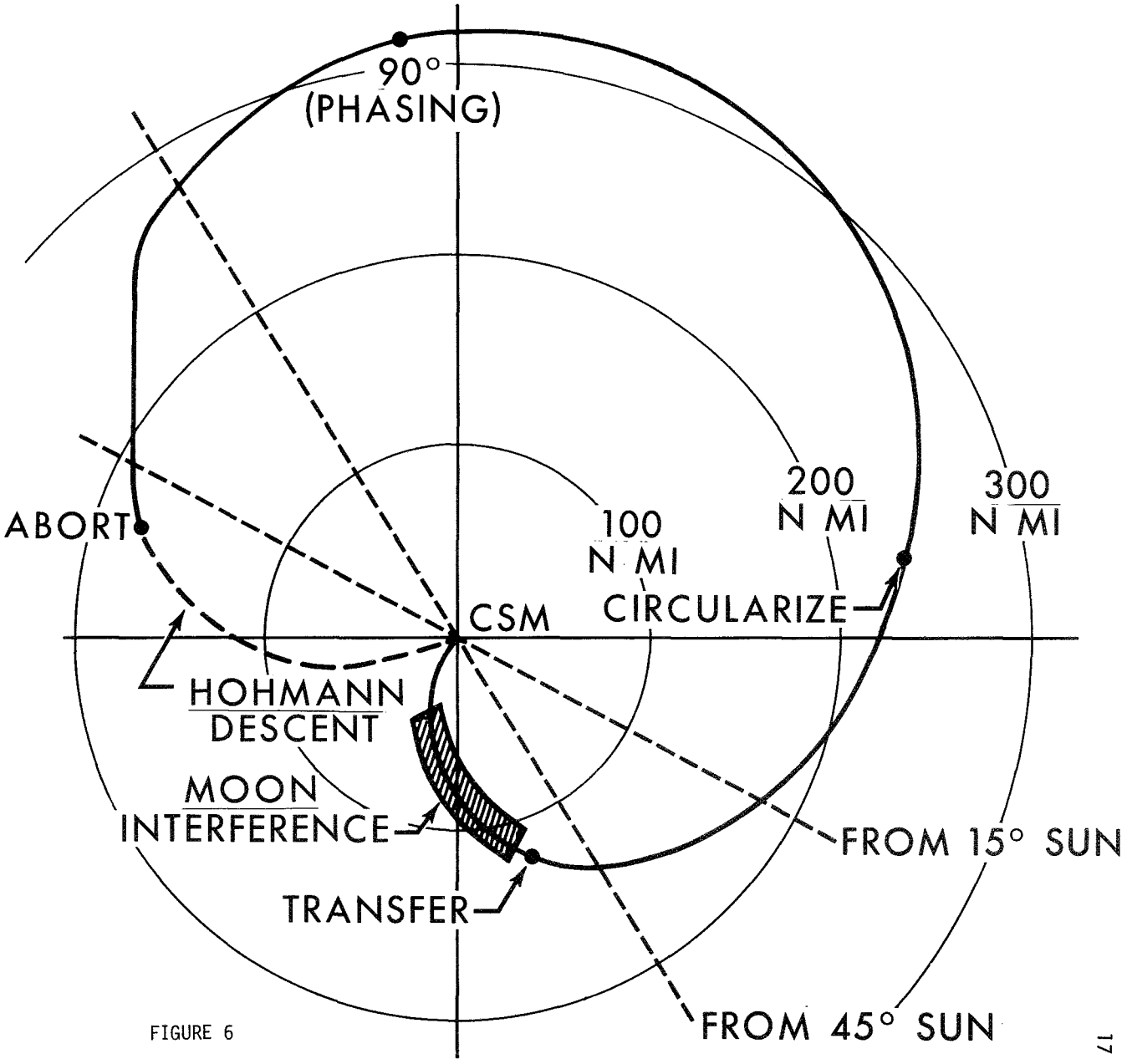

FIGURE 6

NASA-S-66-3125 APR 8

RELATIVE POSITION ERROR FOR AN ABORT 12 MINUTES AFTER LEM-CSM SEPARATION

DIRECT TRANSFER OF 70°
SAMPLING PERIOD = 3 MIN

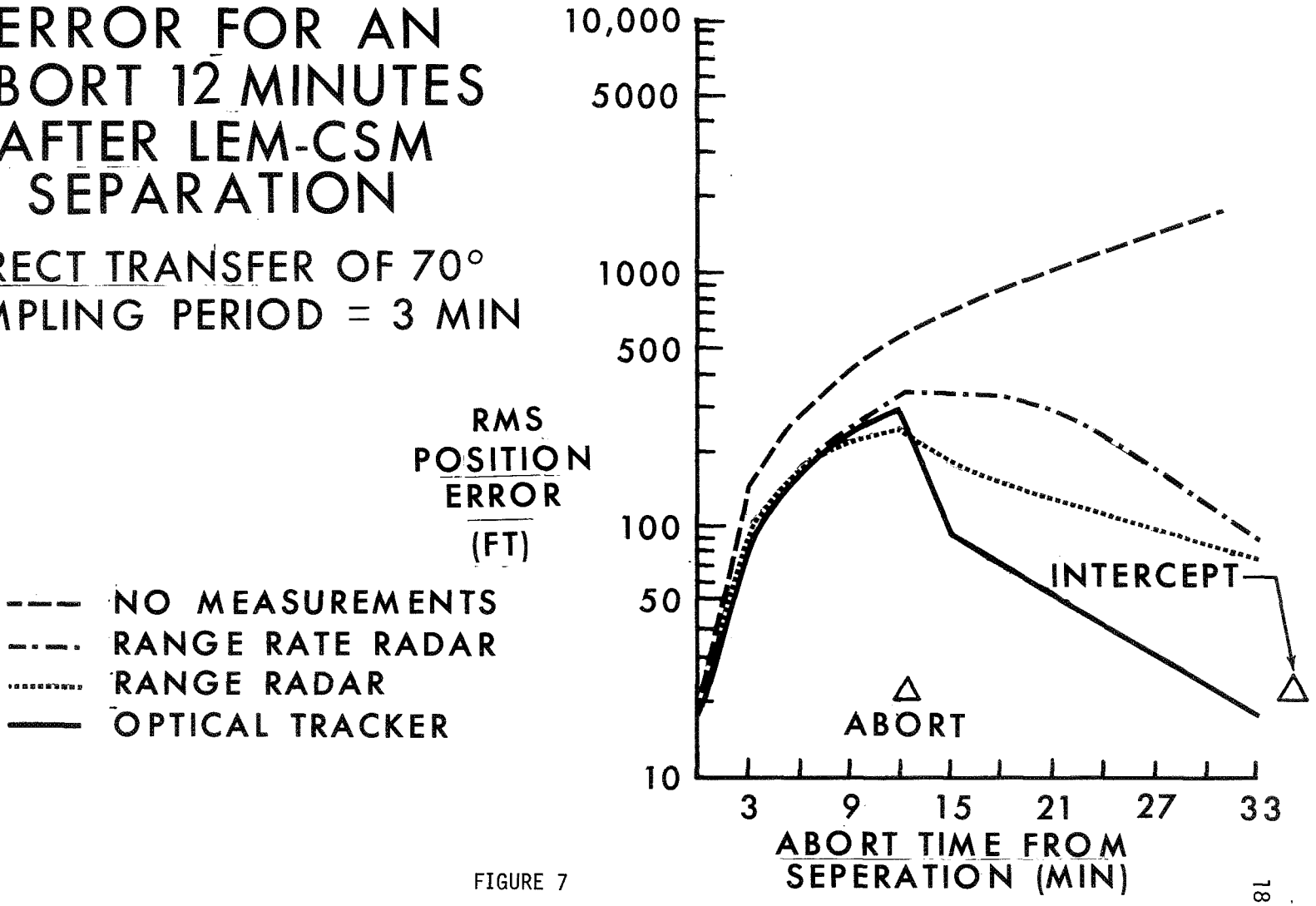

FIGURE 7

NASA-S-66-2988 APR 4

RELATIVE POSITION ERROR FOR AN ABORT 35 MINUTES AFTER LEM-CSM SEPARATION

DIRECT TRANSFER OF 140°
SAMPLING PERIOD = 3 MIN

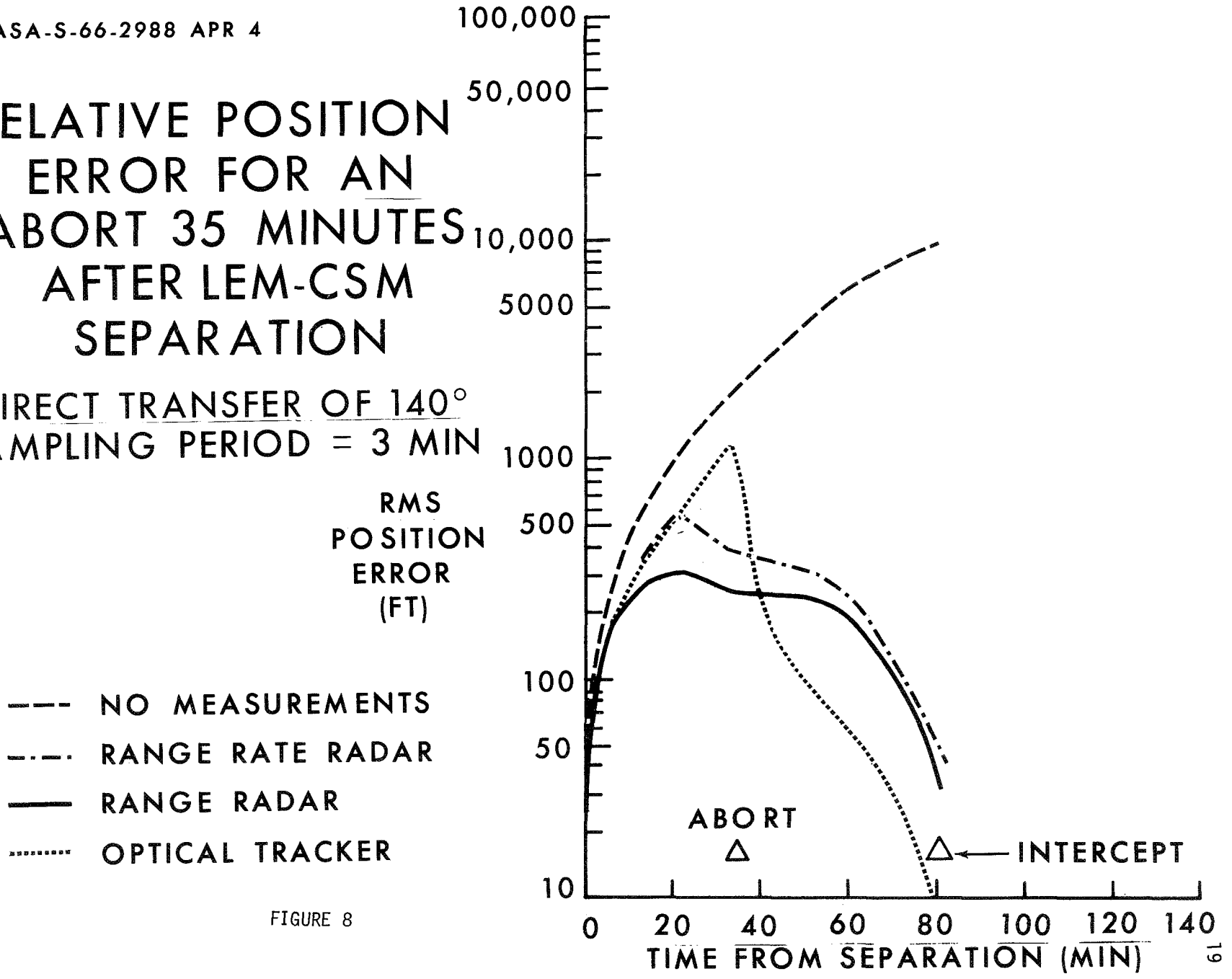

FIGURE 8

NASA-S-66-2969 APR 4

RELATIVE POSITION ERROR (ABORT FROM START OF POWERED DESCENT)

SUN ELEVATION =45°
SAMPLING PERIOD = 3 MIN

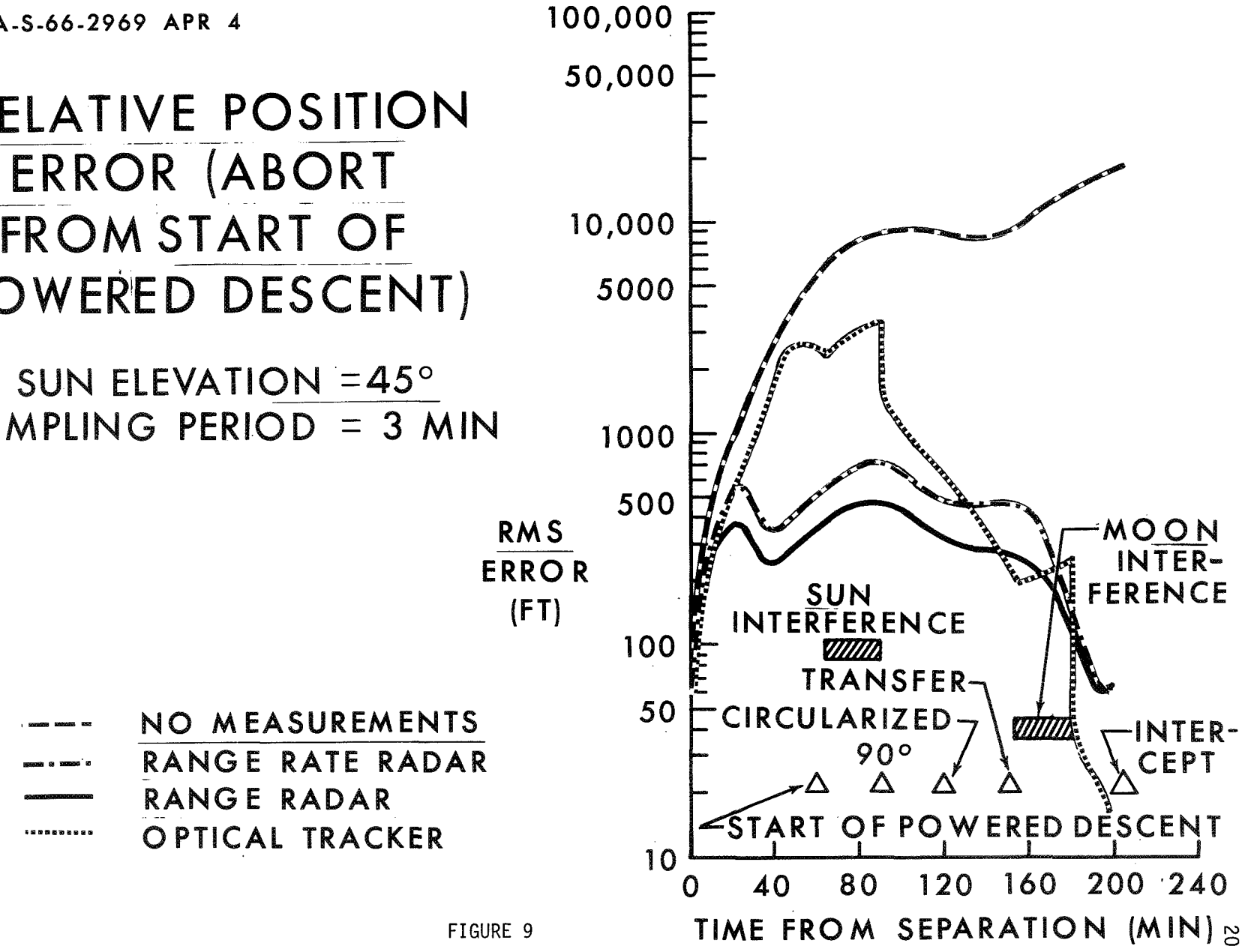

FIGURE 9

NASA-S-66-3001 APR 4

EFFECT OF SAMPLING PERIOD ON RELATIVE POSITION ERROR (NOMINAL LAUNCH)

SUN ELEVATION = 45°
OPTICAL TRACKER

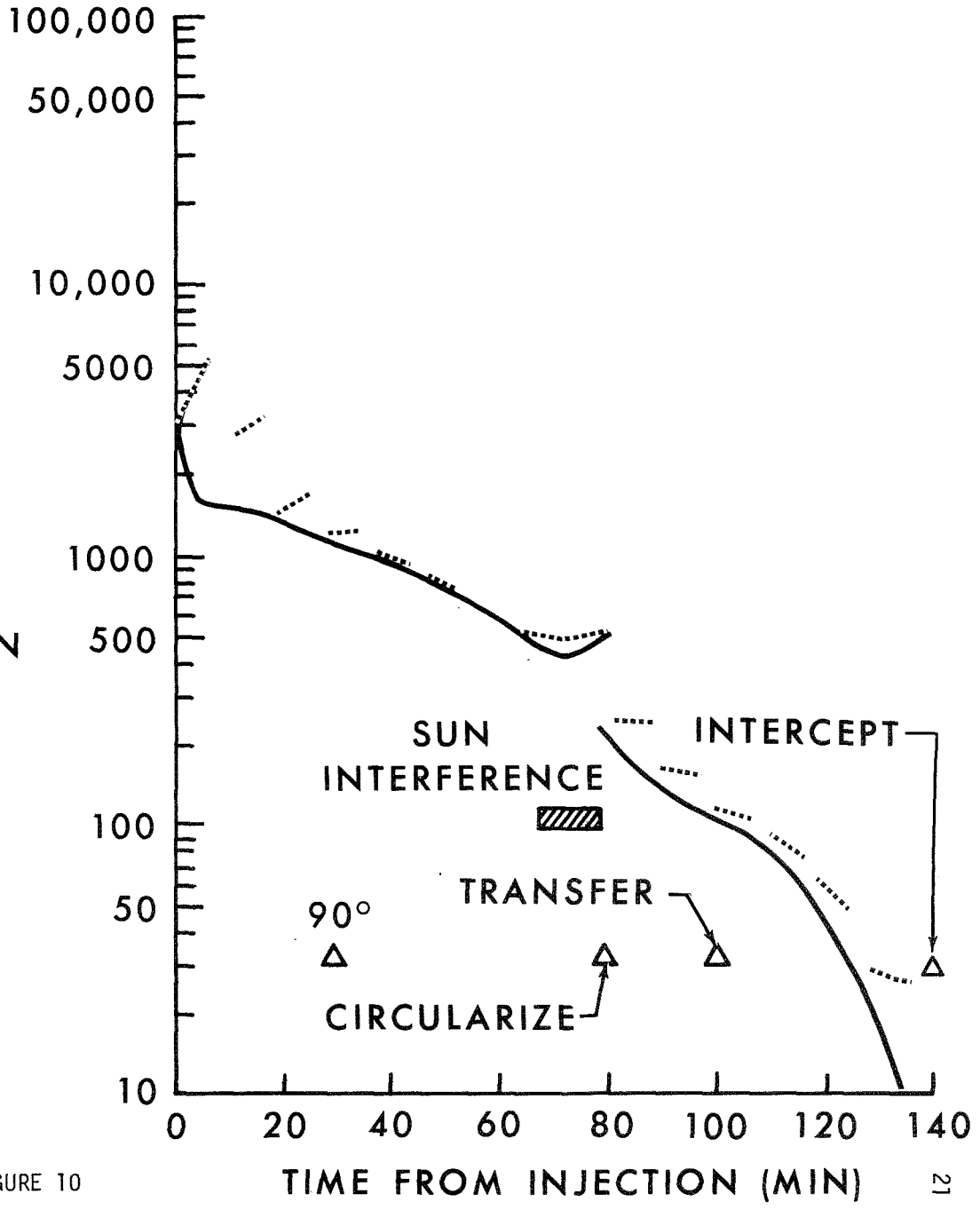

SAMPLING PEROID = TIME BETWEEN MEASUREMENTS

..... 9 MIN SAMPLING

—— 3 MIN SAMPLING

FIGURE 10

NASA-S-66-2971 APR 4

EFFECT OF SAMPLING PERIOD ON RELATIVE POSITION ERROR (NOMINAL LAUNCH)

RANGE RADAR

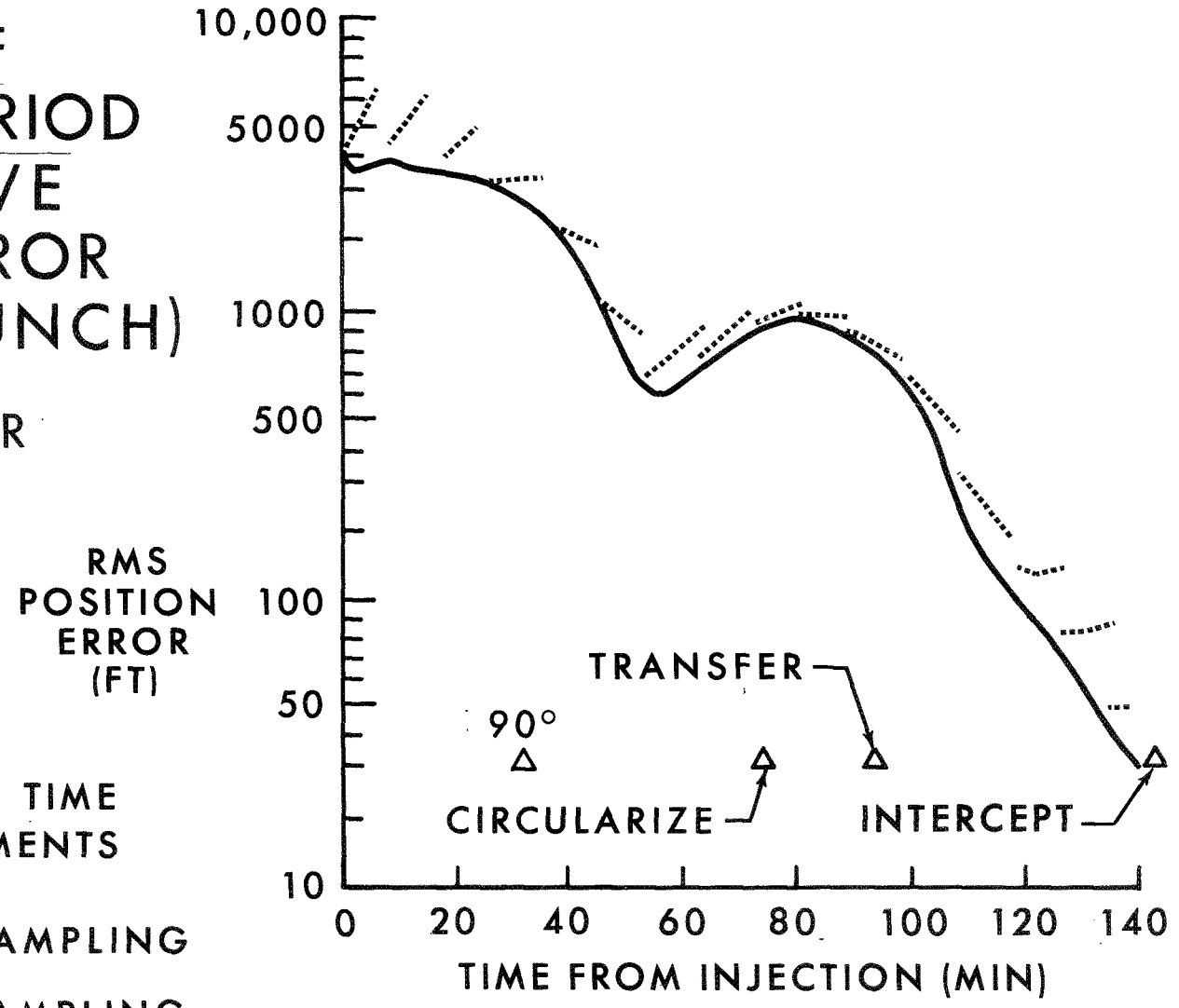

SAMPLING PERIOD = TIME BETWEEN MEASUREMENTS

..... 9 MIN SAMPLING

—— 3 MIN SAMPLING

FIGURE 11

NASA-S-66-3124 APR 8

EFFECT OF OPTICAL TRACKER ACCURACY ON RELATIVE POSITION ERROR (NOMINAL LAUNCH)

SUN ELEVATION = 45°

SAMPLING PERIOD = 3 MIN

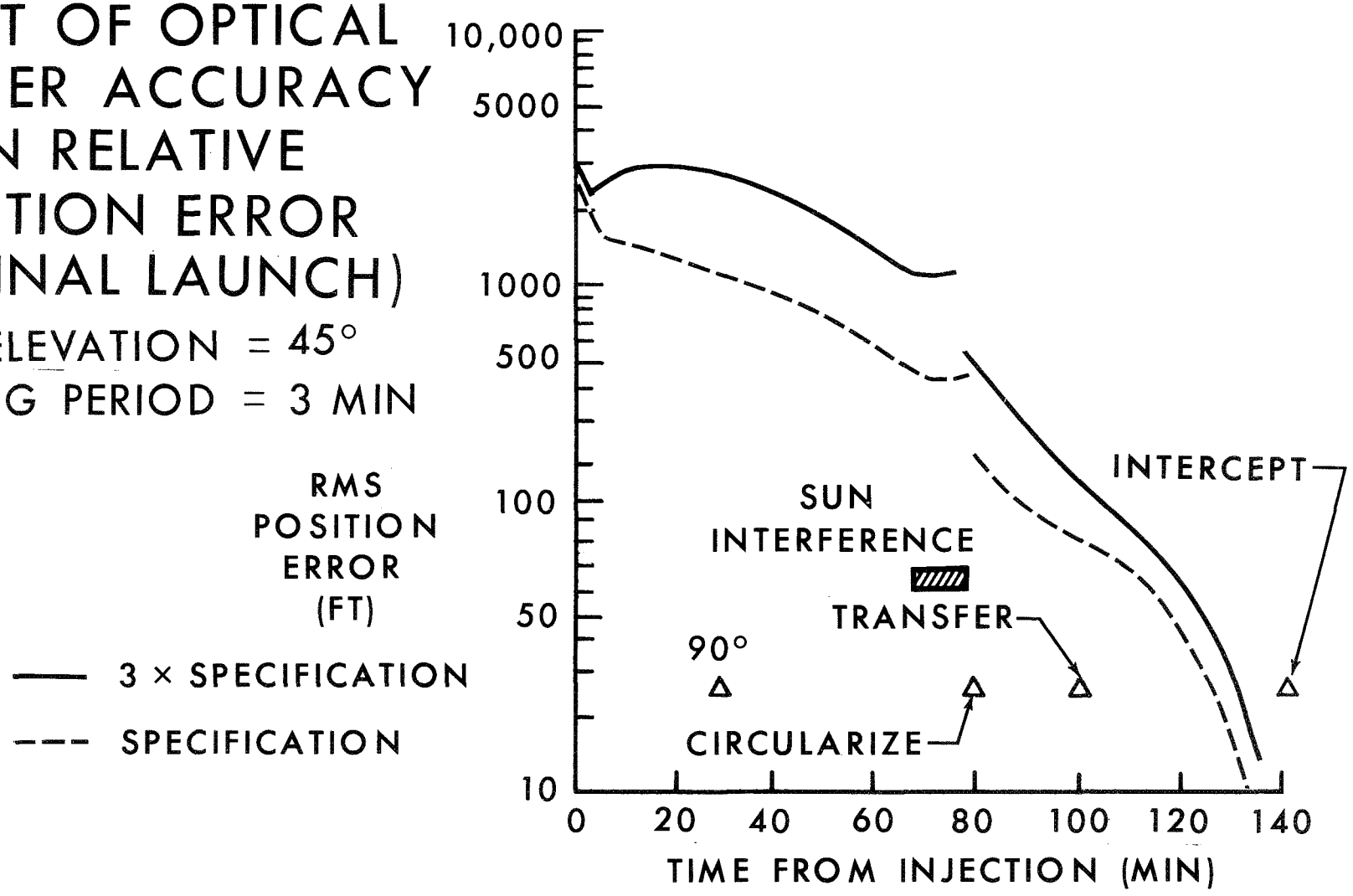

FIGURE 12

NASA-S-66-3113 APR 8

EFFECT OF RANGE RADAR ACCURACY ON RELATIVE POISTION ERROR

NOMINAL LAUNCH SAMPLING PERIOD = 3 MIN

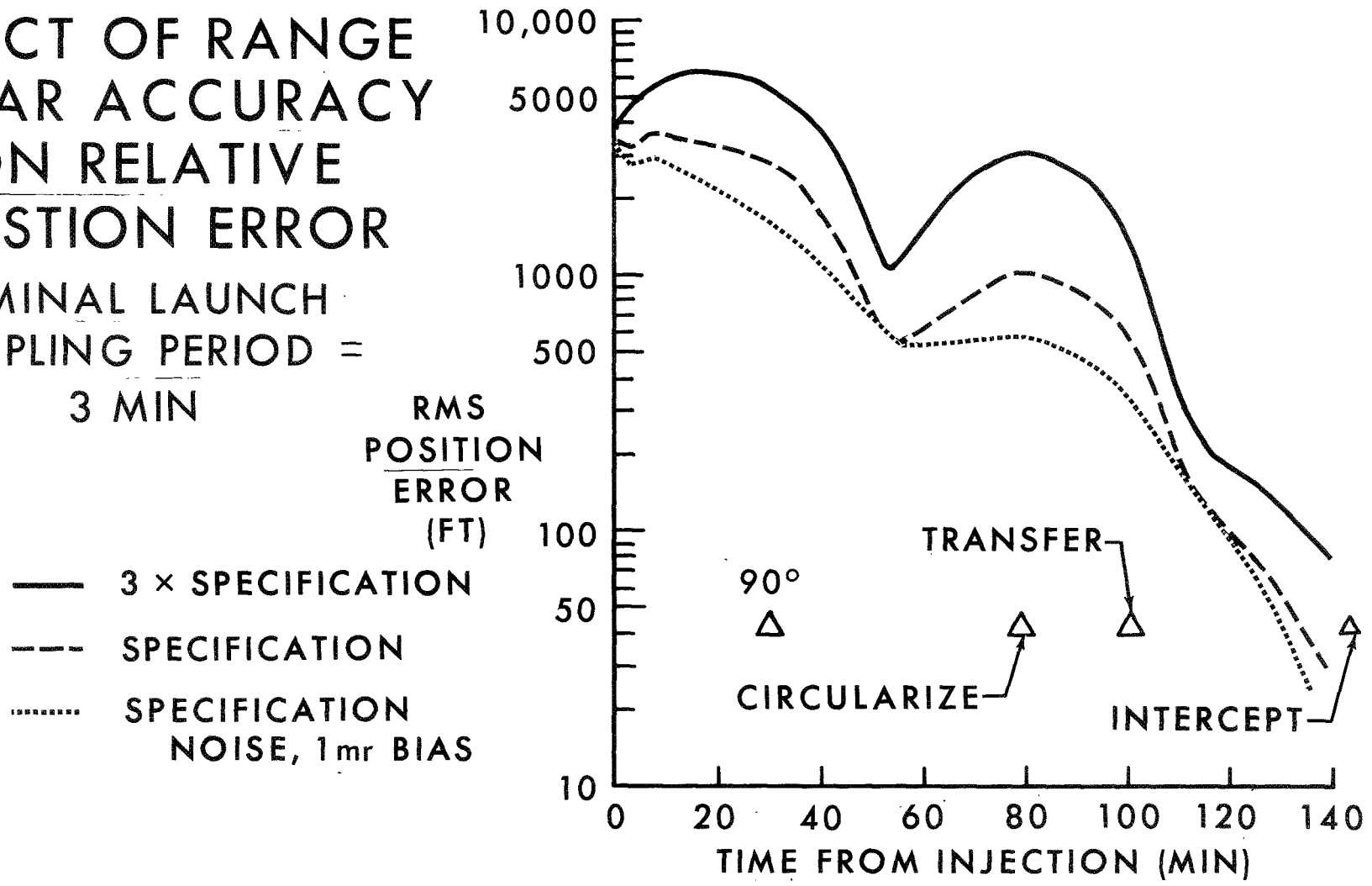

FIGURE 13

NASA-S-66-2977 APR 4

ΔV REQUIRED TO COMPENSATE FOR INJECTION ERRORS

	LOTS	RR/AOT
NOMINAL LAUNCH (FT/SEC)	$\mu = 0.6$	$\mu = 2.7$
	$\sigma = 1.8$	$\sigma = 4.4$
LATE LAUNCH (FT/SEC)	$\mu = 8.7$	$\mu = 10.0$
	$\sigma = 11.0$	$\sigma = 12.4$

FIGURE 14

APPENDIX A

The purpose of this appendix is to describe a computer program which provides the capability to perform error analyses of LEM-CSM rendezvous trajectories. Particular attention has been given to the simulation of the CFP (concentric flight plan), but the basic program has the capability of simulating virtually any type of rendezvous trajectory with only moderate alterations.

For convenience, this appendix is divided into two main sections. The first section is a verbal description of what the program does in terms of what is computed, and how it is computed. The second section presents the appropriate equations which correspond to the description given in the first section.

Description of Program

Dynamics.- The CSM is assumed to be in an orbit about the moon. The equations of motion for the CSM are written relative to an inertial coordinate system centered in the moon, which is assumed to have an inverse square, central force field.

The LEM is assumed to be on a trajectory which would lead to rendezvous with the CSM. The motion of the LEM is described by its position and velocity measured relative to that of the CSM.

A LEM guidance maneuver is represented by simply adding a ΔV to the LEM velocity vector.

Navigation System.- The navigation system is simulated by assuming that measurements would be processed by a Kalman type filter. The use of this filter entails linearization about nominal trajectories, white gaussian noise representation of random input variables, and a certain amount of given a priori statistics.

The program will compute the covariance matrix of the error in the estimate of the deviations from the nominal relative state of the LEM. The corresponding covariance matrix for the CSM is also computed.

Measurements.- Either optical sightings or radar measurements can be simulated. In the case of optical sightings, a measurement consists of the simultaneous reading of two angles plus bias and random errors. Radar measurements consist of the simultaneous reading of two angles, range or range-rate, plus bias and random errors.

The angle measurements programed for the Optical Tracker are azimuth and elevation, as opposed to two gimbal angles for the radar shaft and trunion. In addition, the angular bias errors are assumed to be initially independent, and the noise errors independent unto perpetuity. This is only approximately correct because of the actual angles measured, the IMU misalinement, and the NAV Base misalinement. The drift of the gyros is programed to affect the two biases independently and drifts between integration steps are assumed to be independent. This is sort of a white noise characterization. Additionally, before an V maneuver, the IMU is realined, and the bias estimation initialized.

Of course, measurements are simulated only in the sense of computing their effects on the statistics of the estimation process.

Measurement Constraint.- In simulating measurements made by an optical tracker, it is necessary to consider that the tracker cannot track if the angle between the lines of sight to the sun and to the vehicle is less than some critical value. Moreover, this critical angle is a function of the range between the vehicles. This effect is simulated in the program by prohibiting optical measurements when the constraint is not satisfied.

EQUATIONS FOR THE PROGRAM

Dynamic Equations. The equations of motion for the CSM are given by

$$\ddot{\bar{R}}_c = -\frac{\mu}{r_c^3}\bar{R}_c \tag{1}$$

where

$\bar{R}_C$ = radius vector of CSM

$r_C = \| \bar{R}_C \|$

μ = gravitational constant for moon

Let $\bar{R}_L$ denote the radius vector of LEM and define the relative vector

$$\bar{\rho} = \bar{R}_L - \bar{R}_C \tag{2}$$

The differential equation for $\bar{\rho}$ is

$$\ddot{\bar{\rho}} = -\frac{\mu}{r_L^3}\left\{\bar{\rho} + \left[1 - \left(\frac{r_L}{r_c}\right)^3\right]\bar{R}_c\right\} \tag{3}$$

where

$$r_L = \| \bar{\rho} + \bar{R}_c \|$$

Nominal trajectories (i.e., solutions of (1) and (3) for $\bar{R}_C(t)$ and $\bar{\rho}(t)$) are needed to compute coefficients in the matrix differential equations given in the next section.

Transition Matrices. The transition matrix for CSM deviations is denoted by Φ and computed from

$$\frac{d}{dt}\Phi(t,t_0) = F(t)\Phi(t,t_0) \qquad \Phi(t_0,t_0) = I \tag{4}$$

where

$$F(t) = \begin{bmatrix} 0 & I \\ \alpha^*(t) & 0 \end{bmatrix}$$

and

$$\alpha^*(t) = -\frac{\mu}{r_c^3(t)}\left[I - \frac{3}{r_c^2(t)}\bar{R}_c(t)\bar{R}_c^T(t)\right]$$

with superscription T denoting transpose.

The fundamental matrix for relative deviations is denoted by Φ and computed from

$$\frac{d}{dt}\Phi(t, t_o) = f^*(t)\,\Phi(t, t_o), \quad \Phi(t_o, t_o) = I \qquad (5)$$

where

$$f^*(t) = \begin{bmatrix} 0 & I \\ \beta^*(t) & 0 \end{bmatrix}$$

and

$$\beta^*(t) = \frac{3\mu}{r_L^5}\left\{-\frac{r_L^2}{3} I + (\bar{\rho}+\bar{R}_c)(\bar{\rho}+\bar{R}_c)^T\right\}$$

Since the relative state is a function of the CSM state (see equation (3)), there is the additional transition matrix for relative deviations which is denoted by Γ and computed from

$$\frac{d}{dt}\Gamma(t,t_o) = f^*(t)\Gamma(t,t_o) + g^*(t)\Phi(t,t_o) \qquad \Gamma(t_o,t_o)=0 \qquad (6)$$

where

$$g^*(t) = \begin{bmatrix} \gamma^*(t) & 0 \\ 0 & 0 \end{bmatrix}$$

and

$$\gamma^*(t) = \frac{3\mu}{r_L^5}\left\{\frac{r_L^2}{3}\left(\frac{r_L^3}{r_c^3}-1\right) I + (\bar{\rho}+\bar{R}_c)(\bar{\rho}+\bar{R}_c)^T + \frac{r_L^5}{r_c^5}\bar{R}_c\bar{R}_c^T\right\}$$

CSM Errors. It is assumed that the estimate of the CSM state is not updated during the flight. Therefore, if the error in the estimate at time t_K is denoted by e_K, and if P_K is defined as

$$P_K = E\left\{e_K e_K^T\right\}$$

Then

$$P_{K+1} = \Phi(t_{K+1}, t_K) P_K \Phi^T(t_{K+1}, t_K) \qquad (7)$$

where it is assumed that P_o will be given. It should be noted that if the estimate of the CSM state is the nominal trajectory, then P_K is also the covariance matrix of the CSM dispersions, and the dispersions are the negative of the errors.

Relative State Estimation Errors. The propagation of relative state estimation errors is done in the following way:

I.) Define the matrix M as

$$M_{K+1} = \Phi \Pi_K \Phi^T + \Gamma S_K \Gamma^T + \Gamma P_K \Gamma^T + \Phi Z_K \Gamma^T + \Gamma Z_K^T \Phi^T \quad (8)$$

where the arguments of Φ, Γ and T are (t_{K+1}, t_K), and

$$\Pi_K = E\left\{\epsilon_K \epsilon_K^T\right\}$$

$$Z_K = E\left\{\epsilon_K e_K^T\right\}$$

S_K = Cov. (error in measuring ΔV correction; null if no correction is made)

where

ϵ_K = error in estimating relative state at time t_K.

It should be noted that if Φ is partitioned, i.e.

$$\Phi = \begin{bmatrix} \theta_{11} & \theta_{12} \\ \theta_{21} & \theta_{22} \end{bmatrix}$$

then

$$\Gamma = \begin{bmatrix} \theta_{12} \\ \theta_{22} \end{bmatrix}$$

II.) Compute the gain matrix K from

$$K = M B^T (BMB^T + R)^{-1} \quad (9)$$

where all matrices in (9) are understood to have subscript k+1, and B and R are defined as follows:

a.) If z denotes the vector valued measurement given by

$$z = m(\bar{p}) + V$$

where v is the noise in the measurement, then

b.) The matrix B is a Jacobian matrix, i.e.

$$B = \left[\partial m_i / \partial \rho_j \right]$$

evaluated on the nominal trajectory.

III. Having computed K, the matrices Π and Z are updated by

$$\begin{aligned} \Pi_{K+1} &= (I - KB)M_{K+1} \\ Z_{K+1} &= (I - KB)(\Phi Z_K + \Gamma P_K)\Phi^T \end{aligned} \tag{10}$$

where all matrices without subscripts are understood to have subscript k+1.

The accuracy of the estimation process is obtained from the Π matrix.

Measurement Constraint. The angle between the line of sight to the sun and the line of sight to the CSM is determined by

$$\varphi = \cos^{-1}\left(- \frac{\bar{u}_{sL} \cdot \bar{\rho}}{\| \bar{\rho} \|} \right)$$

where $\bar{u}_{s_1}$ is a unit vector in the direction of the sun. The critical angle, φ^*, is computed from

$$\varphi^* = 5^\circ + 25^\circ \left[1 - e^{-.0154(\rho - 40)} \right]$$

where $\rho \triangleq \| \bar{\rho} \|$ is given in nautical miles.

The criteria which must be met for an optical sighting to be made is as follows:

A. If $\rho < 40$ n.m., make a measurement only if $\varphi > 5^\circ$.

B. If $\rho \geq 40$ n.m., make a measurement only if $\varphi > \varphi^*$.

The expression for φ^* was obtained by fitting a curve to imperical data. Two sets of data were available, one set being the design criteria for the tracker, the other being a 100 factor degradation of the tracker filter performance. The curve is between the two sets of data, but is weighted more in the direction of the degraded performance.